Station-Keeping and Formation Flying Based on Nonlinear Output Regulation Theory

Akiyama, Yuki
Department of Aeronautics and Astronautics, Kyushu University

Bando, Mai
Department of Aeronautics and Astronautics, Kyushu University

Hokamoto, Shinji
Department of Aeronautics and Astronautics, Kyushu University

出版情報：Acta Astronautica. 153, pp.289-296, 2018-12. Elsevier
バージョン：
権利関係：

Station-Keeping and Formation Flying Based on Nonlinear Output Regulation Theory

Yuki Akiyama[a,*], Mai Bando[a], Shinji Hokamoto[a]

[a] *Department of Aeronautics and Astronautics, Kyushu University, 744 Motooka, Nishu-ku, Fukuoka 819-0395, Japan*

Abstract

Station-keeping and formation flying along a libration point orbit in the circular restricted three-body problem are considered. In order to deal with the relative motion with respect to a reference trajectory, this paper extends our previous study which derives the station-keeping controller based on the output regulation theory. First the reference orbit of the chief satellite is represented as the output of an autonomous system called exosystem, assuming the reference orbit is given by a truncated Fourier series. For the formation flying, the relative trajectory of the deputy satellite with respect to the chief satellite is also represented by the output of an exosystem. Then the reference signal to be asymptotically tracked for the formation flying is obtained by the superposition of the two exosystems. The proposed controllers are applied and verified for the station-keeping and formation flying along a periodic orbit of the Sun-Earth L_2 point.

Keywords: Station-keeping, Formation Flying, Output Regulation

1. Introduction

Libration points and bounded orbits around them in the circular restricted three-body problem (CRTBP) have been given much attention for long time

☆Fully documented templates are available in the elsarticle package on CTAN.

*Corresponding author

Email addresses: akimaru@aero.kyushu-u.ac.jp (Yuki Akiyama), mbando@aero.kyushu-u.ac.jp (Mai Bando), hokamoto@aero.kyushu-u.ac.jp (Shinji Hokamoto)

since they have attractive properties which the Keplerian motion does not posses. In these decades, several space missions using periodic or quasi-periodic orbits around the collinear libration point have been conducted [1, 2, 3, 4, 5, 6, 7, 8, 9, 10]. The formation flying of multiple satellite around the libration point also has significant space science applications such as deep space interferometry which requires a number of telescopes to maintain formation with very high accuracy [11]. However, the dynamics around the collinear libration point is highly unstable and hence effective methods of station-keeping and formation flying are required to achieve desired missions [12, 13, 14].

Station-keeping and formation flying in the CRTBP have been studied by many authors [15, 16, 17, 18, 19, 20, 21, 22, 23, 24]. Recently, based on the output regulation theory of a linear system [25], a control law to realize formation flying and station-keeping was proposed [26, 27]. However, they utilized the dynamics obtained via feedback linearization, and therefore the control costs for large reference orbits become high due to the nonlinearity.

The purpose of this paper is to propose the station-keeping and formation flying controllers based on the nonlinear output regulation theory [28, 29] as the extension of the works [26, 27] to deal with the relative motion with respect to a reference trajectory. First, a Fourier series approximation is introduced to describe a periodic or quasi-periodic orbit in the CRTBP. By using this approximation, a neutrally stable exosystem to describe a reference trajectory for station-keeping is developed and the explicit solution to the nonlinear output regulation problem is derived. Then, the reference trajectory for formation flying based on the relative motion model is developed by superposing another exosystem which describes a desired motion of the deputy satellite with respect to the chief satellite. As numerical examples, the Sun-Earth CRTBP is considered and the station-keeping and formation flying along a Lyapunov orbit around the L_2 point are demonstrated.

2. Equations of Motion in CRTBP

In the CRTBP, the equations of motion in non-dimensional form [30] are expressed as

$$\begin{aligned} X'' - 2Y' &= \frac{\partial U}{\partial X} + u_x \\ Y'' + 2X' &= \frac{\partial U}{\partial Y} + u_y \\ Z'' &= \frac{\partial U}{\partial Z} + u_z \end{aligned} \tag{1}$$

where $\{X, Y, Z\}$ is the rotating frame whose origin is the barycenter of the system; the coordinates and time are normalized by the distance between the two main bodies and by the period of the circular orbit respectively; $(\cdot)'$ denotes the differentiation of $(\cdot)$ with respect to non-dimensional time t; (u_x, u_y, u_z) is the control acceleration;

$$\begin{aligned} U &= \frac{1-\mu}{r_1} + \frac{\mu}{r_2} + \frac{1}{2}\left(X^2 + Y^2\right) \\ r_1 &= \sqrt{(X+\mu)^2 + Y^2 + Z^2} \\ r_2 &= \sqrt{(X-1+\mu)^2 + Y^2 + Z^2} \end{aligned}$$

where $\mu = M_2/(M_1 + M_2)$; and M_1 and M_2 are the masses of the two main bodies with $M_1 > M_2$.

Equation (1) has libration points known as Lagrangian points L_i satisfying

$$\frac{\partial U}{\partial X} = \frac{\partial U}{\partial Y} = \frac{\partial U}{\partial Z} = 0 \tag{2}$$

and the Lagrangian points are expressed as

$$\begin{aligned} &L_1 = (l_1(\mu), 0, 0), \quad L_2 = (l_2(\mu), 0, 0), \quad L_3 = (l_3(\mu), 0, 0) \\ &L_4 = (1/2 - \mu, \sqrt{3}/2, 0), \quad L_5 = (1/2 - \mu, -\sqrt{3}/2, 0) \end{aligned}$$

where $l_i(\mu)$ are determined by setting $Y = 0$ and solving $\dfrac{\partial U}{\partial X} = 0$. To describe the motion near a collinear libration point L_i $(i = 1, 2, 3)$, it is convenient to use a coordinate system $\{x, y, z\}$ with its origin at L_i. Replacing $\{X, Y, Z\}$ with

$\{x + l_i, y, z\}$ and rewriting Eq. (1) in the state space form yields

$$\boldsymbol{x}' = \boldsymbol{f}(\boldsymbol{x}) + \boldsymbol{B}\boldsymbol{u} \tag{3}$$

where $\boldsymbol{x} = \begin{bmatrix} \boldsymbol{r}^{\mathrm{T}} & \boldsymbol{r}'^{\mathrm{T}} \end{bmatrix}^{\mathrm{T}}$, $\boldsymbol{r} = \begin{bmatrix} x & y & z \end{bmatrix}^{\mathrm{T}}$, $\boldsymbol{u} = \begin{bmatrix} u_x & u_y & u_z \end{bmatrix}^{\mathrm{T}}$, $\boldsymbol{B} = \begin{bmatrix} \boldsymbol{O}_3 & \boldsymbol{I}_3 \end{bmatrix}^{\mathrm{T}}$ and

$$\boldsymbol{f}(\boldsymbol{x}) = \begin{bmatrix} \boldsymbol{r}' \\ \nabla U(\boldsymbol{r}) + \boldsymbol{K}\boldsymbol{r}' \end{bmatrix}, \quad \boldsymbol{K} = \begin{bmatrix} 0 & 2 & 0 \\ -2 & 0 & 0 \\ 0 & 0 & 0 \end{bmatrix}$$

3. Nonlinear Output Regulation Problem

The nonlinear output regulation theory is reviewed in this section. The detailed description can be found in [28, 29].

The output regulation problem for a general nonlinear system is modeled by

$$\dot{\boldsymbol{x}} = \boldsymbol{f}(\boldsymbol{x}, \boldsymbol{u}, \boldsymbol{w}) \tag{4}$$

$$\boldsymbol{e} = \boldsymbol{h}(\boldsymbol{x}, \boldsymbol{u}, \boldsymbol{w}) \tag{5}$$

$$\dot{\boldsymbol{w}} = \boldsymbol{s}(\boldsymbol{w}) \tag{6}$$

where state $\boldsymbol{x} \in \mathbb{R}^n$, control input $\boldsymbol{u} \in \mathbb{R}^m$, exogenous signal $\boldsymbol{w} \in \mathbb{R}^q$ and regulated output $\boldsymbol{e} \in \mathbb{R}^r$. Equation (4) is a plant, and the exogenous signal $\boldsymbol{w}$ is generated by an external autonomous system (6), which is called an exosystem. Assuming that $\boldsymbol{f} : \mathbb{R}^n \times \mathbb{R}^m \times \mathbb{R}^q \to \mathbb{R}^n$, $\boldsymbol{h} : \mathbb{R}^n \times \mathbb{R}^m \times \mathbb{R}^q \to \mathbb{R}^r$ and $\boldsymbol{s} : \mathbb{R}^q \to \mathbb{R}^q$ are C^k $(k \geq 2)$, and also that $\boldsymbol{f}(\boldsymbol{0}, \boldsymbol{0}, \boldsymbol{0}) = \boldsymbol{0}$, $\boldsymbol{h}(\boldsymbol{0}, \boldsymbol{0}, \boldsymbol{0}) = \boldsymbol{0}$ and $\boldsymbol{s}(\boldsymbol{0}) = \boldsymbol{0}$. Moreover, the plant (4) and the exosystem (6) satisfy the following assumptions: The pair $\left(\frac{\partial \boldsymbol{f}}{\partial \boldsymbol{x}}(\boldsymbol{0}, \boldsymbol{0}, \boldsymbol{0}), \frac{\partial \boldsymbol{f}}{\partial \boldsymbol{u}}(\boldsymbol{0}, \boldsymbol{0}, \boldsymbol{0})\right)$ is stabilizable and the exosystem (6) is neutrally stable, which are necessary conditions to solve the following local output regulation problem.

The local output regulation problem is to find a stabilizing feedback control law such that $\boldsymbol{e} \to \boldsymbol{0}$ as time goes to infinity for any initial state in a vicinity sufficiently close to $(\boldsymbol{x}(0), \boldsymbol{w}(0)) = (\boldsymbol{0}, \boldsymbol{0})$. This problem is solvable if and only if

there exist mappings $\boldsymbol{\pi}(\boldsymbol{w})$ and $\boldsymbol{c}(\boldsymbol{w})$ with $\boldsymbol{\pi}(\boldsymbol{0}) = \boldsymbol{0}$ and $\boldsymbol{c}(\boldsymbol{0}) = \boldsymbol{0}$ which satisfy the conditions [28]:

$$\frac{\partial \boldsymbol{\pi}(\boldsymbol{w})}{\partial \boldsymbol{w}} \boldsymbol{s}(\boldsymbol{w}) = \boldsymbol{f}(\boldsymbol{\pi}(\boldsymbol{w}), \boldsymbol{c}(\boldsymbol{w}), \boldsymbol{w}) \tag{7}$$

$$\boldsymbol{0} = \boldsymbol{h}(\boldsymbol{\pi}(\boldsymbol{w}), \boldsymbol{c}(\boldsymbol{w}), \boldsymbol{w}) \tag{8}$$

These solvability conditions guarantee that the regulated output for the closed-loop system consisting of Eqs. (4) and (6) tends to zero as time goes to infinity. Equation (7) is the condition that the closed-loop composite system has a center manifold $\boldsymbol{x} = \boldsymbol{\pi}(\boldsymbol{w})$, and Eq. (8) implies that the regulated output for the system lying on the center manifold is zero.

Finally, an admissible feedback control law is given by

$$\boldsymbol{u} = -\boldsymbol{F}(\boldsymbol{x} - \boldsymbol{\pi}(\boldsymbol{w})) + \boldsymbol{c}(\boldsymbol{w}) \tag{9}$$

where $\boldsymbol{F}$ is an arbitrary matrix such that $\left(\frac{\partial \boldsymbol{f}}{\partial \boldsymbol{x}}(\boldsymbol{0}, \boldsymbol{0}, \boldsymbol{0}) - \frac{\partial \boldsymbol{f}}{\partial \boldsymbol{u}}(\boldsymbol{0}, \boldsymbol{0}, \boldsymbol{0})\boldsymbol{F}\right)$ is stable.

4. Station-Keeping and Formation Flying Controller

In this section, the station-keeping and formation flying problems are formulated as tracking problems and the output regulation theory is applied to solve the problems.

4.1. Station-Keeping Controller

The station-keeping on a libration point orbit is considered. Let $\boldsymbol{x}$ be the state of a satellite, $\boldsymbol{x}^C$ be the reference orbit, and $\boldsymbol{x}_n^C$ be the n-th order approximation of $\boldsymbol{x}^C$. Assuming that the projection of the reference trajectory onto each coordinate is a periodic function, the position vector of $\boldsymbol{x}_n^C$,

$\boldsymbol{r}_n^C = \left[\begin{array}{ccc} x_n^C & y_n^C & z_n^C \end{array} \right]^{\mathrm{T}}$, is given by

$$\begin{aligned} x_n^C(t) &= a_{x0}^C + \sum_{k=1}^{n} (a_{xk}^C \cos k\omega_x^C t + b_{xk}^C \sin k\omega_x^C t) \\ y_n^C(t) &= a_{y0}^C + \sum_{k=1}^{n} (a_{yk}^C \cos k\omega_y^C t + b_{yk}^C \sin k\omega_y^C t) \\ z_n^C(t) &= a_{z0}^C + \sum_{k=1}^{n} (a_{zk}^C \cos k\omega_z^C t + b_{zk}^C \sin k\omega_z^C t) \end{aligned} \tag{10}$$

where ω_x^C, ω_y^C, and ω_z^C are angular frequencies of the reference orbit projected onto each coordinate. In general, these frequencies are not the same values, thereby Eq. (10) represents a quasi-periodic orbit. As a special case of $\omega_x^C = \omega_y^C = \omega_z^C$, Eq. (10) becomes a periodic orbit.

The exosystem generating the reference orbit (10) is expressed as a linear state space form:

$$\boldsymbol{w}_n' = \boldsymbol{S}_n \boldsymbol{w}_n, \quad \boldsymbol{w}_n(0) = \boldsymbol{w}_0 \tag{11}$$

where

$$\boldsymbol{w}_n = \left[\begin{array}{ccc} \boldsymbol{w}_{x,n}^{\mathrm{T}} & \boldsymbol{w}_{y,n}^{\mathrm{T}} & \boldsymbol{w}_{z,n}^{\mathrm{T}} \end{array} \right]^{\mathrm{T}} \in \mathbb{R}^{3(2n+1)} \tag{12}$$

$$\boldsymbol{w}_{j,n} = \left[\begin{array}{c|cc|cc|c|cc} w_{j,0} & w_{j,1} & \bar{w}_{j,1} & w_{j,2} & \bar{w}_{j,2} & \cdots & w_{j,n} & \bar{w}_{j,n} \end{array} \right]^{\mathrm{T}} \quad (j = x, y, z) \tag{13}$$

$$\boldsymbol{w}_0 = \left[\begin{array}{ccc} \boldsymbol{w}_{x0}^{\mathrm{T}} & \boldsymbol{w}_{y0}^{\mathrm{T}} & \boldsymbol{w}_{z0}^{\mathrm{T}} \end{array} \right]^{\mathrm{T}} \in \mathbb{R}^{3(2n+1)} \tag{14}$$

$$\boldsymbol{w}_{j0} = \left[\begin{array}{c|cc|cc|c|cc} a_{j0}^C & a_{j1}^C & b_{j1}^C & a_{j2}^C & b_{j2}^C & \cdots & a_{jn}^C & b_{jn}^C \end{array} \right]^{\mathrm{T}} \quad (j = x, y, z) \tag{15}$$

$$\boldsymbol{S}_n = \mathrm{diag} \left[\begin{array}{ccc} \omega_x^C & \omega_y^C & \omega_z^C \end{array} \right] \otimes \mathrm{diag} \left[\begin{array}{ccccccc} 0 & \boldsymbol{J} & 2\boldsymbol{J} & \cdots & n\boldsymbol{J} \end{array} \right] \in \mathbb{R}^{3(2n+1)\times 3(2n+1)} \tag{16}$$

$$\boldsymbol{J} = \left[\begin{array}{cc} 0 & 1 \\ -1 & 0 \end{array} \right] \tag{17}$$

and $\otimes$ denotes the Kronecker product. It should be noted that the solutions to

the system of differential equations (11) are given by

$$\begin{cases} w_{j,0}(t) = a_{j0}^C & (k=0) \\ \begin{cases} w_{j,k}(t) = a_{jk}^C \cos k\omega_j^C t + b_{jk}^C \sin k\omega_j^C t \\ \bar{w}_{j,k}(t) = -a_{jk}^C \sin k\omega_j^C t + b_{jk}^C \cos k\omega_j^C t \end{cases} & (1 \le k \le n) \end{cases}$$

for $j = x, y, z$. Hence, the reference orbit (10) are expressed as the superposition of $w_{j,k}$ as

$$x_n^C(t) = \sum_{k=0}^{n} w_{x,k} = \boldsymbol{L}_n \boldsymbol{w}_{x,n},\ y_n^C(t) = \sum_{k=0}^{n} w_{y,k} = \boldsymbol{L}_n \boldsymbol{w}_{y,n},\ z_n^C(t) = \sum_{k=0}^{n} w_{z,k} = \boldsymbol{L}_n \boldsymbol{w}_{z,n} \tag{18}$$

where

$$\boldsymbol{L}_n = \left[\ 1 \ \middle|\ 1 \quad 0 \ \middle|\ 1 \quad 0 \ \middle|\ \cdots \ \middle|\ 1 \quad 0\ \right] \in \mathbb{R}^{2n+1} \tag{19}$$

and the output to regulate is defined as

$$\boldsymbol{e} = \boldsymbol{r} - \boldsymbol{r}_n^C = \boldsymbol{r} - \boldsymbol{D}_n \boldsymbol{w}_n \tag{20}$$

with $\boldsymbol{D}_n = \boldsymbol{I}_3 \otimes \boldsymbol{L}_n \in \mathbb{R}^{3\times 3(2n+1)}$.

For Eqs. (3), (11) and (20), the mappings to solve Eq. (7) and (8) are explicitly given by

$$\boldsymbol{\pi}_n(\boldsymbol{w}_n) = \begin{bmatrix} \boldsymbol{D}_n \\ \boldsymbol{D}_n \boldsymbol{S}_n \end{bmatrix} \boldsymbol{w}_n \triangleq \boldsymbol{\Pi}_n \boldsymbol{w}_n \tag{21}$$

$$\boldsymbol{c}_n(\boldsymbol{w}_n) = -\nabla U(\boldsymbol{D}_n \boldsymbol{w}_n) + (\boldsymbol{D}_n \boldsymbol{S}_n - \boldsymbol{K}\boldsymbol{D}_n)\, \boldsymbol{S}_n \boldsymbol{w}_n \triangleq -\nabla U(\boldsymbol{D}_n \boldsymbol{w}_n) + \boldsymbol{\Gamma}_n \boldsymbol{w}_n \tag{22}$$

By replacing $\boldsymbol{\pi}(\boldsymbol{w})$ and $\boldsymbol{c}(\boldsymbol{w})$ in Eq. (9) by Eqs. (21) and (22), the controller for the n^{th} order problem is obtained as

$$\boldsymbol{u}^C = -\boldsymbol{F}(\boldsymbol{x} - \boldsymbol{\Pi}_n \boldsymbol{w}_n) - \nabla U(\boldsymbol{D}_n \boldsymbol{w}_n) + \boldsymbol{\Gamma}_n \boldsymbol{w}_n \tag{23}$$

The controller (23) can achieve asymptotic tracking for the n-th order problem for any initial state in a vicinity sufficiently close to $(\boldsymbol{x}(0), \boldsymbol{w}_n(0)) = (\boldsymbol{0}, \boldsymbol{0})$.

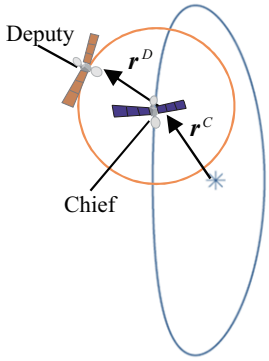

Figure 1: Formation Flying: the chief is orbiting a periodic orbit and the deputy is orbiting around the chief.

Moreover, the station-keeping cost of control input evaluated in the absolute integral, *i.e.* L_1 norm, can be made arbitrarily small by taking n sufficiently large (See Appendix). The structure of the controller (23) can be understood by dividing into two parts: a linear feedback term $-\boldsymbol{F}(\boldsymbol{x}-\boldsymbol{\Pi}_n\boldsymbol{w}_n)$ and remaining terms $-\nabla U(\boldsymbol{D}_n\boldsymbol{w}_n)+\boldsymbol{\Gamma}_n\boldsymbol{w}_n$. The latter part locally linearizes the system in the vicinity of the reference orbit, and the linear feedback locally stabilizes the error system.

4.2. Formation Flying Controller

Let us consider the formation flying of two satellites as shown in Fig. 1: the chief satellite on a libration point orbit and the deputy satellite orbiting around the chief satellite. In the following, the formation flying controller for the deputy satellite is derived. Let $\boldsymbol{x}$ be the state of the deputy satellite, $\boldsymbol{x}^D = \boldsymbol{x} - \boldsymbol{x}^C$ be the reference orbit of the deputy satellite with respect to the chief satellite, and $\boldsymbol{x}_n^D$ be the n-th order approximation of $\boldsymbol{x}^D$. The relative position vector of $\boldsymbol{x}_n^D$,

$\boldsymbol{r}_n^D = \begin{bmatrix} x_n^D & y_n^D & z_n^D \end{bmatrix}^{\mathrm{T}}$, is given by

$$\begin{aligned} x_n^D(t) &= a_{x0}^D + \sum_{k=1}^{n}(a_{xk}^D \cos k\omega_x^D t + b_{xk}^D \sin k\omega_x^D t) \\ y_n^D(t) &= a_{y0}^D + \sum_{k=1}^{n}(a_{yk}^D \cos k\omega_y^D t + b_{yk}^D \sin k\omega_y^D t) \\ z_n^D(t) &= a_{z0}^D + \sum_{k=1}^{n}(a_{zk}^D \cos k\omega_z^D t + b_{zk}^D \sin k\omega_z^D t) \end{aligned} \tag{24}$$

where a_{jk}^D, b_{jk}^D and ω_j^D are the Fourier coefficients and the frequencies of the reference orbit for the deputy satellite, respectively. Note that the Fourier series (24) are used to represent an arbitrary order quasi-periodic orbit.

Similar to the station-keeping problem, the exosystem generating Eq. (24) is given by

$$\boldsymbol{v}_n' = \boldsymbol{S}_n \boldsymbol{v}_n, \quad \boldsymbol{v}_n(0) = \boldsymbol{v}_0 \tag{25}$$

where

$$\boldsymbol{v}_n = \begin{bmatrix} \boldsymbol{v}_{x,n}^{\mathrm{T}} & \boldsymbol{v}_{y,n}^{\mathrm{T}} & \boldsymbol{v}_{z,n}^{\mathrm{T}} \end{bmatrix}^{\mathrm{T}} \in \mathbb{R}^{3(2n+1)} \tag{26}$$

$$\boldsymbol{v}_{j,n} = \left[\begin{array}{c|c|c|c|c|c} v_{j,0} & v_{j,1} & \bar{v}_{j,1} & v_{j,2} & \bar{v}_{j,2} & \cdots \end{array}\right. \left.\begin{array}{c|c} v_{j,n} & \bar{v}_{j,n} \end{array}\right]^{\mathrm{T}} \quad (j = x, y, z) \tag{27}$$

$$\boldsymbol{v}_0 = \begin{bmatrix} \boldsymbol{v}_{x0}^{\mathrm{T}} & \boldsymbol{v}_{y0}^{\mathrm{T}} & \boldsymbol{v}_{z0}^{\mathrm{T}} \end{bmatrix}^{\mathrm{T}} \in \mathbb{R}^{3(2n+1)} \tag{28}$$

$$\boldsymbol{v}_{j0} = \left[\begin{array}{c|c|c|c|c|c} a_{j0}^D & a_{j1}^D & b_{j1}^D & a_{j2}^D & b_{j2}^D & \cdots \end{array}\right. \left.\begin{array}{c|c} a_{jn}^D & b_{jn}^D \end{array}\right]^{\mathrm{T}} \quad (j = x, y, z) \tag{29}$$

$$\boldsymbol{S}_n = \mathrm{diag}\begin{bmatrix} \omega_x^D & \omega_y^D & \omega_z^D \end{bmatrix} \otimes \mathrm{diag}\begin{bmatrix} 0 & \boldsymbol{J} & 2\boldsymbol{J} & \cdots & n\boldsymbol{J} \end{bmatrix} \in \mathbb{R}^{3(2n+1)\times 3(2n+1)} \tag{30}$$

Then, the reference orbit Eq. (24) are expressed as

$$x_n^D(t) = \sum_{k=0}^{n} v_{x,k} = \boldsymbol{L}_n \boldsymbol{v}_{x,n}, \; y_n^D(t) = \sum_{k=0}^{n} v_{y,k} = \boldsymbol{L}_n \boldsymbol{v}_{y,n}, \; z_n^D(t) = \sum_{k=0}^{n} v_{z,k} = \boldsymbol{L}_n \boldsymbol{v}_{z,n} \tag{31}$$

The goal of the output regulation problem is asymptotic tracking of $\boldsymbol{r}_{n_c}^C + \boldsymbol{r}_{n_d}^D$, where n_c and n_d denote the truncation order of reference orbit for the chief and deputy satellites, respectively. Then, the exosystem generating the reference

orbit $\boldsymbol{r}_{n_c}^C + \boldsymbol{r}_{n_d}^D$ of the deputy satellite with respect to L_i is simply expressed as the superposition of two exosystems Eqs. (11) and (25) as

$$\boldsymbol{y}' = \boldsymbol{U}\boldsymbol{y} \tag{32}$$

where $\boldsymbol{y} = \begin{bmatrix} \boldsymbol{w}_{n_c}^{\mathrm{T}} & \boldsymbol{v}_{n_d}^{\mathrm{T}} \end{bmatrix}^{\mathrm{T}} \in \mathbb{R}^{6(n_c+n_d+1)}$, $\boldsymbol{U} = \mathrm{diag}\begin{bmatrix} \boldsymbol{S}_{n_c} & \boldsymbol{S}_{n_d} \end{bmatrix} \in \mathbb{R}^{6(n_c+n_d+1)\times 6(n_c+n_d+1)}$. The output to regulate is defined as

$$\boldsymbol{e} = \boldsymbol{r} - \left(\boldsymbol{r}_{n_c}^C + \boldsymbol{r}_{n_d}^D\right) = \boldsymbol{C}\boldsymbol{x} - \left(\boldsymbol{D}_{n_c}\boldsymbol{w}_{n_c} + \boldsymbol{D}_{n_d}\boldsymbol{v}_{n_d}\right) = \boldsymbol{C}\boldsymbol{x} - \boldsymbol{D}\boldsymbol{y} \tag{33}$$

where $\boldsymbol{D} = \begin{bmatrix} \boldsymbol{D}_{n_c} & \boldsymbol{D}_{n_d} \end{bmatrix} \in \mathbb{R}^{3\times 6(n_c+n_d+1)}$. Then, the mappings to solve Eqs. (7) and (8) are explicitly given by

$$\boldsymbol{\pi}(\boldsymbol{y}) = \begin{bmatrix} \boldsymbol{D} \\ \boldsymbol{D}\boldsymbol{U} \end{bmatrix} \boldsymbol{y} \triangleq \boldsymbol{\Pi}\boldsymbol{y} \tag{34}$$

$$\boldsymbol{c}(\boldsymbol{y}) = -\nabla U(\boldsymbol{D}\boldsymbol{y}) + (\boldsymbol{D}\boldsymbol{U} - \boldsymbol{K}\boldsymbol{D})\,\boldsymbol{U}\boldsymbol{y} \triangleq -\nabla U(\boldsymbol{D}\boldsymbol{y}) + \boldsymbol{\Gamma}\boldsymbol{y} \tag{35}$$

where $\boldsymbol{\Pi} \in \mathbb{R}^{6\times 6(n_c+n_d+1)}$ and $\boldsymbol{\Gamma} \in \mathbb{R}^{3\times 6(n_c+n_d+1)}$.

By replacing $\boldsymbol{\pi}(\boldsymbol{w})$ and $\boldsymbol{c}(\boldsymbol{w})$ in Eq. (9) by Eqs. (34) and (35), the controller for formation flying is obtained as

$$\boldsymbol{u}^D = -\boldsymbol{F}\left(\boldsymbol{x} - \boldsymbol{\Pi}\boldsymbol{y}\right) - \nabla U(\boldsymbol{D}\boldsymbol{y}) + \boldsymbol{\Gamma}\boldsymbol{y} \tag{36}$$

The controller (36) can achieve formation flying for any initial state in a vicinity sufficiently close to $(\boldsymbol{x}(0), \boldsymbol{y}(0)) = (\boldsymbol{0}, \boldsymbol{0})$. Similar to the station-keeping controller (23), the terms $-\nabla U(\boldsymbol{D}\boldsymbol{y}) + \boldsymbol{\Gamma}\boldsymbol{y}$ in Eq. (36) locally linearize the system in the vicinity of the reference orbit, and the linear feedback locally stabilizes the error system between the states of spacecraft and the reference orbit. Further, setting $\boldsymbol{v}_{n_d} = \boldsymbol{0}$, Eq. (36) strictly accords with Eq. (23) and achieves station-keeping along a (quasi-)periodic orbit generated by the exosignal $\boldsymbol{w}_{n_c}$. Therefore, the controller (36) is more general form than the station-keeping controller (23) since it can be utilized for both station-keeping and formation flying. It should be noted that although the reference trajectory for formation flying is simply expressed as the linear superposition, the formation flying controller (36)

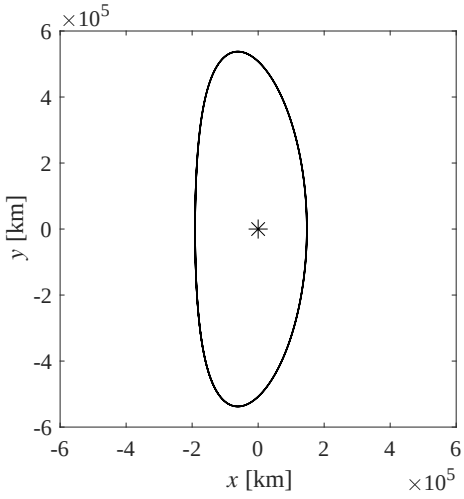

Figure 2: Pseudo-periodic orbit ($n = 8$).

derived by solving the nonlinear output regulation takes into account the nonlinear effect due to the difference between the position vectors of the chief and deputy satellites.

5. Simulation Results for Sun-Earth CRTBP

In this section, the control laws (23) and (36) are applied to the nonlinear equations of motion (1) for the Sun-Earth CRTBP. First, station-keeping on a Lyapunov orbit is considered to verify the controller (23). Then, formation flying along the Lyapunov orbit is demonstrated by using the controller (36). In the simulations, Lagrangian point is specified as L_2. The period of the orbit and the radius of the Sun-Earth system are set to be $T_0 = 365.26$ days and $R_0 = 1.4960 \times 10^8$ km, respectively. Then, other parameters are specified as $\mu = 3.0542 \times 10^{-6}$, $l_2 = 1.0101$ and $\sigma_2 = 3.9393$. The initial condition for a Lyapunov orbit in the normalized units is given by

$$\boldsymbol{x}_0^C = \begin{bmatrix} -1.2770 & 0 & 0 & 0 & 7.6802 & 0 \end{bmatrix}^{\mathrm{T}} \times 10^{-3} \tag{37}$$

and its period is $T = 3.0843$ (179.17 days).

Table 1: Coefficients and frequencies of Fourier series ($n = 1 \cdots 8$).

Parameter	Value	Parameter	Value
a_{x0}^C	-2.6115e-04	a_{y0}^C	-2.9385e-15
a_{x1}^C	-1.1430e-03	a_{y1}^C	-3.7106e-15
b_{x1}^C	-3.4561e-15	b_{y1}^C	3.6035e-03
a_{x2}^C	1.1392e-04	a_{y2}^C	-1.8178e-15
b_{x2}^C	-3.0444e-15	b_{y2}^C	6.0876e-05
a_{x3}^C	1.1106e-05	a_{y3}^C	-9.4442e-16
b_{x3}^C	-2.4462e-15	b_{y3}^C	1.2130e-05
a_{x4}^C	1.8423e-06	a_{y4}^C	-4.8410e-16
b_{x4}^C	-2.0014e-15	b_{y4}^C	1.6546e-06
a_{x5}^C	2.9137e-07	a_{y5}^C	-2.8570e-16
b_{x5}^C	-1.6741e-15	b_{y5}^C	2.7980e-07
a_{x6}^C	5.0518e-08	a_{y6}^C	-2.0777e-16
b_{x6}^C	-1.4219e-15	b_{y6}^C	4.7852e-08
a_{x7}^C	8.9827e-09	a_{y7}^C	-1.7146e-16
b_{x7}^C	-1.2455e-15	b_{y7}^C	8.6109e-09
a_{x8}^C	1.6508e-09	a_{y8}^C	-1.3221e-16
b_{x8}^C	-1.1039e-15	b_{y8}^C	1.5858e-09
ω_x^C	2.0372	ω_y^C	2.0372

Note that the numerical solution with the initial condition (37) is not exactly periodic, and that it would diverge within a few periods. To represent the Lyapunov orbit in an analytical form, the time history of the position vector for one period is expanded in the Fourier series of order 8. The orbit approximated by the truncated Fourier series with $n = 8$ is shown in Fig. 2 and it is referred to as "*pseudo-periodic orbit*". In addition, the coefficients and frequencies up to $n = 8$ are shown in Table 1. The initial condition obtained for the pseudo-periodic orbit $\boldsymbol{x}_n^C(0)$ is slightly different from Eq. (37) due to the truncation error of Fourier series.

The stabilizing feedback gain $\boldsymbol{F}$ for the feedback term in the derived controllers (23) and (36) can be arbitrary chosen. Here, it is designed by the linear quadratic regulator (LQR) theory as $\boldsymbol{F} = \boldsymbol{R}^{-1}\boldsymbol{B}^{\mathrm{T}}\boldsymbol{P}$, where $\boldsymbol{P}$ is the solution to the algebraic Ricatti equation

$$\boldsymbol{A}^{\mathrm{T}}\boldsymbol{P} + \boldsymbol{P}\boldsymbol{A} + \boldsymbol{Q} - \boldsymbol{P}\boldsymbol{B}\boldsymbol{R}^{-1}\boldsymbol{B}^{\mathrm{T}}\boldsymbol{P} = \boldsymbol{O}_6$$

where $\boldsymbol{Q} = \boldsymbol{I}_6$ and $\boldsymbol{R} = \boldsymbol{I}_3$ in the following simulations.

5.1. Station-Keeping on Libration Orbits

The initial state of the spacecraft is set to L_2 (*i.e.* $\boldsymbol{x}_0 = \boldsymbol{0}$) and the coefficients and frequencies up to $n = 8$ are used to obtain the exosystem. The trajectory controlled by Eq. (23) is shown in Fig. 3 and the time history of the control input and its enlargement are shown in Fig. 4 and Fig. 5, respectively. Figure 3 shows that the controlled state asymptotically tracks the pseudo-periodic orbit. Moreover, it can be seen from Figs. 4 and 5 that the input gets smaller as time passes and becomes periodic. This is because that the state $\boldsymbol{x}_n$ approaches $\boldsymbol{\Pi}_n\boldsymbol{w}_n$ and the input $\boldsymbol{u}$ converges to $-\nabla U(\boldsymbol{\Pi}_n\boldsymbol{w}_n) + \boldsymbol{\Gamma}_n\boldsymbol{w}_n$ as $t \to \infty$. The results suggest that the domain of attraction is large enough to achieve station-keeping along the Lyapunov orbit.

Two performance indices are considered: ΔV_0 and ΔV_1. The definition of ΔV_0 is the L_1 norm of the input until the time T_{conv} when the distance from the reference trajectory becomes smaller than a specific value ε. Another index, ΔV_1, is defined as the L_1 norm of the input for one-period after time T_{conv}, that is,

$$\Delta V_0 = \int_0^{T_{conv}} |\boldsymbol{u}(t)|dt \tag{38}$$

$$\Delta V_1 = \int_{T_{conv}}^{T_{conv}+T} |\boldsymbol{u}(t)|dt \tag{39}$$

Here, ΔV_0 and ΔV_1 evaluated for the truncation order n are shown in Figs. 6 and 7 respectively. Figures 6 and 7 show that ΔV_0 approaches a specific value while ΔV_1 converges to zero as n increases. This is because the higher order approxi-

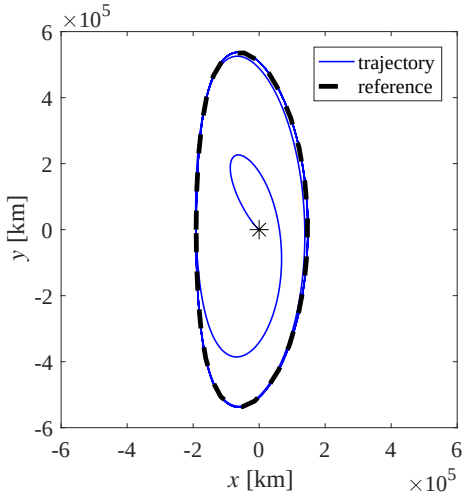

Figure 3: Controlled trajectory ($n = 8$): the solid and dashed lines are the controlled trajectory and the reference orbit, respectively.

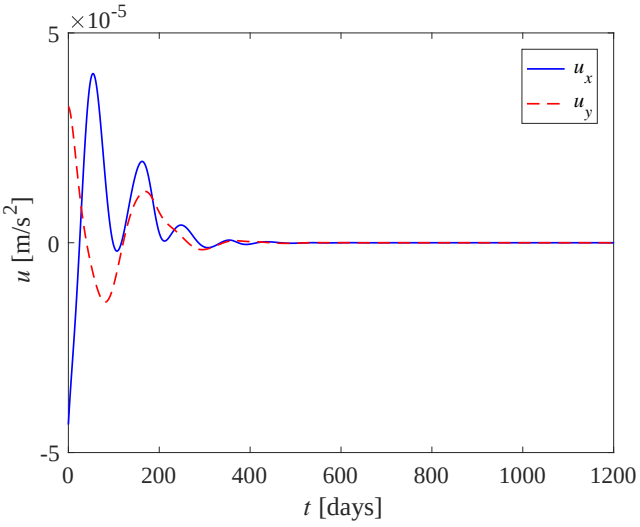

Figure 4: Time history of input ($n = 8$).

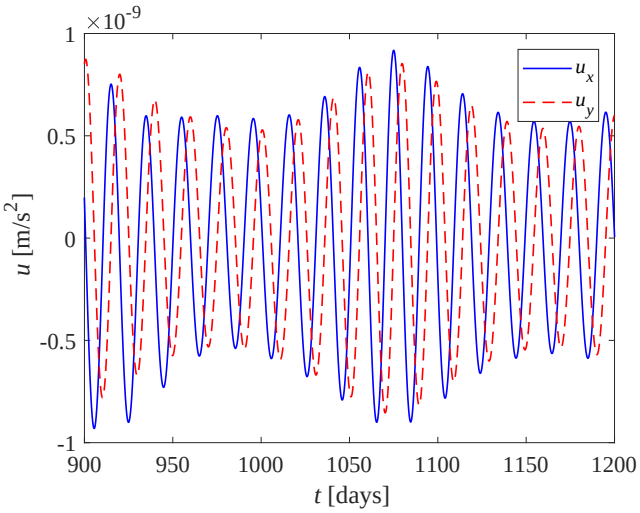

Figure 5: Time history of input ($n = 8$) (enlargement).

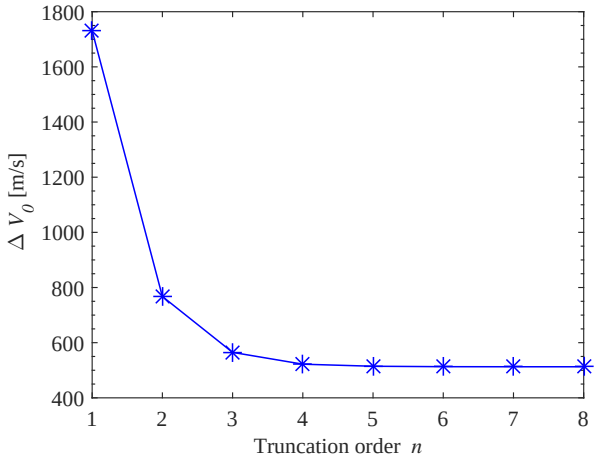

Figure 6: Relation between n and ΔV_0 ($\varepsilon = 1.0000 \times 10^{-7}$).

mation generates a closer orbit to the free motion, and hence, the control effort for station-keeping approaches zero.

Next, we investigate the initial phase dependence on ΔV_0 by exploiting the analytic representation of the reference orbit. For this purpose, the phase dif-

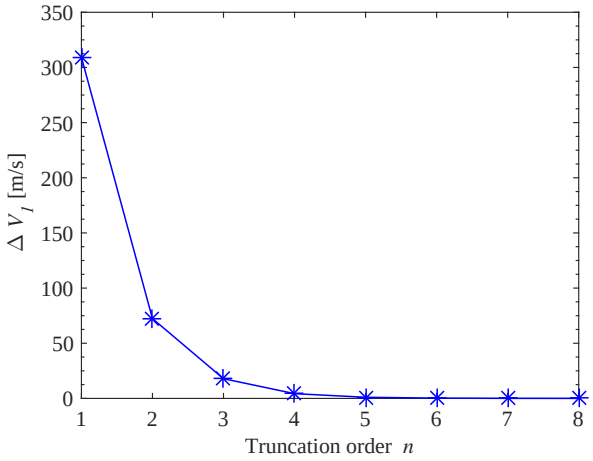

Figure 7: Relation between n and ΔV_1 ($\varepsilon = 1.0000 \times 10^{-7}$).

ference α is incorporated into a Fourier series representation Eq. (10) as

$$\begin{aligned} x_n^C(t;\alpha) &= a_{x0}^C + \sum_{k=1}^{n} \left[\tilde{a}_{xk}(\alpha) \cos k\omega_x^C t + \tilde{b}_{xk}(\alpha) \sin k\omega_x^C t \right] \\ y_n^C(t;\alpha) &= a_{y0}^C + \sum_{k=1}^{n} \left[\tilde{a}_{yk}(\alpha) \cos k\omega_y^C t + \tilde{b}_{yk}(\alpha) \sin k\omega_y^C t \right] \\ z_n^C(t;\alpha) &= a_{z0}^C + \sum_{k=1}^{n} \left[\tilde{a}_{zk}(\alpha) \cos k\omega_z^C t + \tilde{b}_{zk}(\alpha) \sin k\omega_z^C t \right] \end{aligned} \tag{40}$$

where

$$\begin{bmatrix} \tilde{a}_{jk} \\ \tilde{b}_{jk} \end{bmatrix} = \begin{bmatrix} \cos k\alpha & \sin k\alpha \\ -\sin k\alpha & \cos k\alpha \end{bmatrix} \begin{bmatrix} a_{jk}^C \\ b_{jk}^C \end{bmatrix}, \quad (j = x, y, z) \tag{41}$$

The initial positions $\boldsymbol{r}_n^C(0;\alpha) = \boldsymbol{D}_n \boldsymbol{w}_n(0;\alpha)$ for some α are shown in Fig. 8 and the ΔV_0 is evaluated as a function of α in Fig. 9. Figure 9 shows that the ΔV_0 strongly depends on the initial phase of the reference orbit (the minimum value is 369.72 m/s at $\alpha = 294$ deg and the maximum value is 548.90 m/s at $\alpha = 28$ deg in this example).

5.2. Formation flying along a Lyapunov orbit

Formation flying along a Lyapunov orbit is demonstrated. Let us consider that a chief satellite is orbiting the Lyapunov orbit by the controller (23) and one

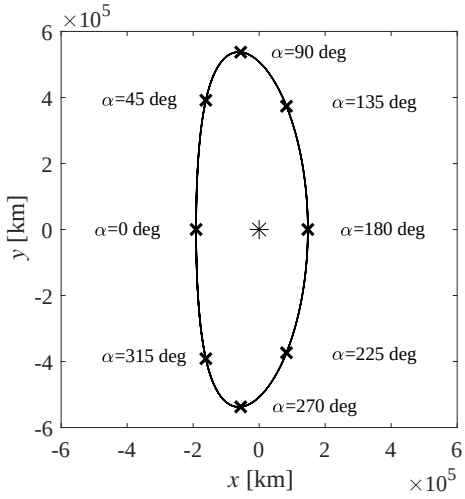

Figure 8: Initial position $\boldsymbol{r}_n^0$ for α.

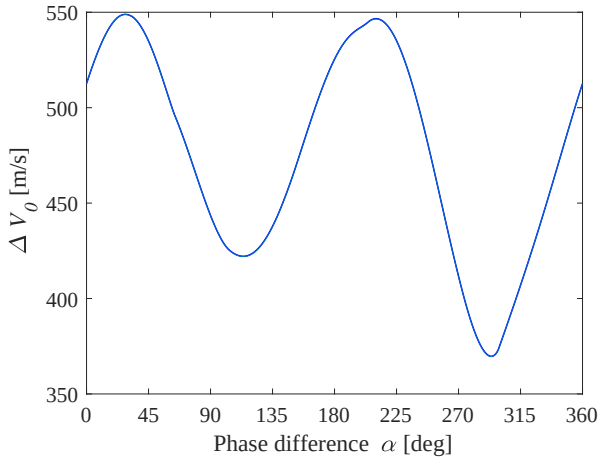

Figure 9: Relation between α and ΔV_0 ($n = 8$).

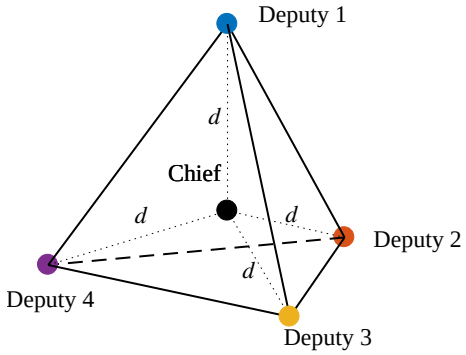

Figure 10: Formation flying constellation: the chief and deputies are at the centroid and the apexes of the regular tetrahedron, respectively.

or more deputy satellites fly in formation with the chief satellite. As examples, we demonstrate two types of formation flying: regular tetrahedron constellation and Lissajous-type formation flying. In the following examples, the pseudo
130 Lyapunov orbit shown in Fig. 2 is used as the chief's reference orbit and deputy satellites are assumed to be initially on the same orbit.

First, the regular tetrahedron constellation is demonstrated. To form the regular tetrahedron constellation as shown in Fig. 10, the chief and four deputies are to be located at the centroid and the apexes of a regular tetrahedron, respectively. Therefore, the position vectors of the deputies $\boldsymbol{r}^{D_i} \quad (i = 1, 2, 3, 4)$ are represented by 0th order Fourier series $\boldsymbol{r}_0^{D_i}$ as:

$$
\begin{aligned}
\boldsymbol{r}_0^{D_1} &= \left[\begin{array}{ccc} 0 & 0 & d \end{array} \right]^{\mathrm{T}} \\
\boldsymbol{r}_0^{D_2} &= \left[\begin{array}{ccc} 0 & \dfrac{2\sqrt{2}}{3}d & -\dfrac{1}{3}d \end{array} \right]^{\mathrm{T}} \\
\boldsymbol{r}_0^{D_3} &= \left[\begin{array}{ccc} \dfrac{\sqrt{6}}{3}d & -\dfrac{\sqrt{2}}{3}d & -\dfrac{1}{3}d \end{array} \right]^{\mathrm{T}} \\
\boldsymbol{r}_0^{D_4} &= \left[\begin{array}{ccc} -\dfrac{\sqrt{6}}{3}d & -\dfrac{\sqrt{2}}{3}d & -\dfrac{1}{3}d \end{array} \right]^{\mathrm{T}}
\end{aligned}
$$

where d is the distance between the chief and the deputies.

The controlled trajectories for $d = 100$ km are shown in Fig. 11. Figure 11(a) shows the trajectories of deputies with respect to the L_2 and Fig. 11(b)

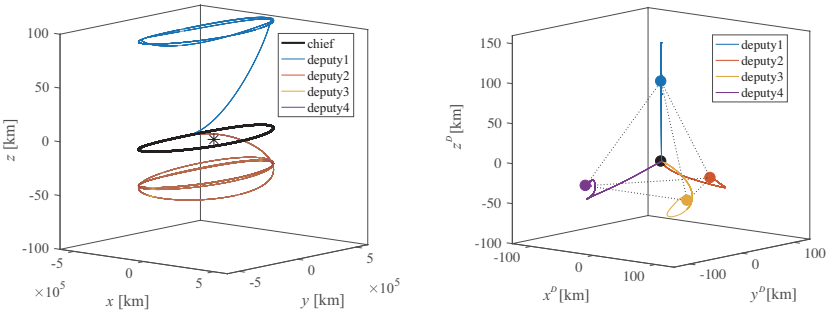

(a) Trajectories 3-D view (b) Relative trajectories of the deputies

Figure 11: Controlled trajectory for the regular tetrahedron constellation.

shows those with respect to the chief. In Fig. 11, all deputies asymptotically tracks the apexes of the regular tetrahedron. Note that the trajectories of the deputies 2 to 4 almost overlap in Fig. 11(a).

Next, the Lissajous-type formation flying is demonstrated. Let us consider that the deputy orbits the Lissajous orbit relative to the chief. As an example, the deputy's relative orbit is given by the 1-st order Fourier series as

$$\boldsymbol{r}_1^D = \begin{bmatrix} r\cos\omega^D t & r\sin 2\omega^D t & r\cos\sqrt{3}\omega^D t \end{bmatrix}^{\mathrm{T}}$$

where r denotes the amplitude of the deputy's relative orbit projected onto each relative coordinate.

Setting $r = 100$ km and $\omega^D = \omega_x^C = 2.0372$, the controlled trajectories of the chief and deputy are shown in Fig. 12. Figure 12(a) shows the trajectories of the chief and deputy with respect to the L_2 and Figs. 12(b) - 12(d) show the trajectories of the deputy with respect to the chief. In Fig. 12, the deputy successfully converges to the Lissajous orbit relative to the chief.

6. Conclusion

Novel station-keeping and formation flying controllers in the circular restricted three-body problem have been proposed based on the nonlinear output

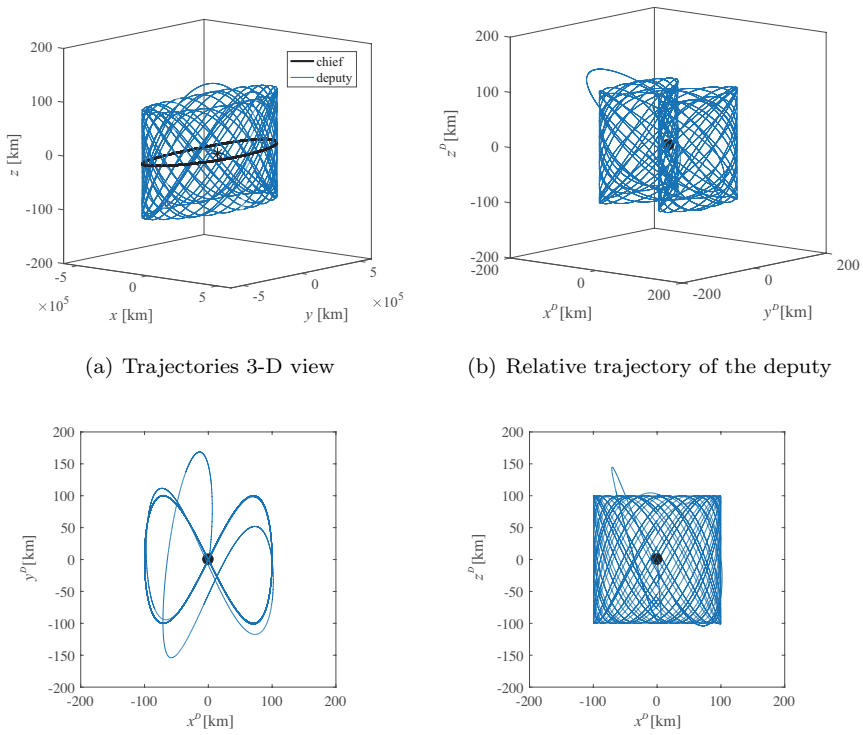

(a) Trajectories 3-D view

(b) Relative trajectory of the deputy

(c) Projection of the relative trajectory onto the x^D-y^D plane

(d) Projection of the relative trajectory onto the x^D-z^D plane

Figure 12: Controlled trajectory for Lissajous-type formation flying.

regulation theory. First the reference orbit of the chief is represented by the output of an exosystem, assuming the reference orbit is represented by a truncated Fourier series. Then the output regulation problem for nonlinear systems was explicitly solved. By the superposition of two exosystems, the formation flying controller was also derived by solving a nonlinear output regulation problem. The proposed station-keeping and formation flying controllers have been verified in numerical simulations for the Lyapunov orbit of the Sun-Earth L_2 point. When a natural orbit is used as a reference orbit and the truncation order is sufficiently large, the proposed station-keeping controller results in very small control cost. Moreover, the examples of formation flying problems show that the proposed controller can deal with various complex formation flying problem

in one framework.

Appendix

Relation between truncation order and total control input

First, it is shown that the state $\boldsymbol{x}$ becomes arbitrarily close to the given reference trajectory $\boldsymbol{x}^C$ by choosing sufficiently large n and t. The asymptotic convergence of the output to zero ($\boldsymbol{e} \to \boldsymbol{0}$) implies $|\boldsymbol{x}(t) - \boldsymbol{x}_n^C(t)| \to 0$ as $t \to \infty$. From the inequality

$$|\boldsymbol{x}(t) - \boldsymbol{x}^C(t)| \leq |\boldsymbol{x}(t) - \boldsymbol{x}_n^C(t)| + |\boldsymbol{x}_n^C(t) - \boldsymbol{x}^C(t)| \tag{.1}$$

and the property of the Fourier series approximation, $|\boldsymbol{x}(t) - \boldsymbol{x}^C(t)| \to 0$ for sufficiently large n and t.

Next, it is shown that $\Delta V = \int_t^{t+T} |\boldsymbol{u}_n^C(t)| dt$ can be arbitrarily small by choosing sufficiently large n and t where T is the period of the reference orbit. From the facts $\boldsymbol{\Pi}_n \boldsymbol{w}_n = \boldsymbol{x}_n^C$ and $\boldsymbol{\Gamma}_n \boldsymbol{w}_n = \boldsymbol{r}_n^{C\prime\prime} - \boldsymbol{K}\boldsymbol{r}_n^{C\prime}$, Eq. (23) can be deformed as

$$\boldsymbol{u}_n^C = -\boldsymbol{F}(\boldsymbol{x} - \boldsymbol{x}_n^C) - \left[\nabla U(\boldsymbol{r}_n^C) - \nabla U(\boldsymbol{r}^C)\right] + \left(\boldsymbol{r}_n^{C\prime\prime} - \boldsymbol{r}^{C\prime\prime}\right) + \boldsymbol{K}\left(\boldsymbol{r}_n^{C\prime} - \boldsymbol{r}^{C\prime}\right) \tag{.2}$$

Then from the inequality

$$|\boldsymbol{u}_n^C| \leq \|\boldsymbol{F}\||\boldsymbol{x} - \boldsymbol{x}_n^C| + |\nabla U(\boldsymbol{r}_n^C) - \nabla U(\boldsymbol{r}^C)| + |\boldsymbol{r}^{C\prime\prime} - \boldsymbol{r}_n^{C\prime\prime}| + \|\boldsymbol{K}\||\boldsymbol{r}_n^{C\prime} - \boldsymbol{r}^{C\prime}| \tag{.3}$$

$|\boldsymbol{u}_n^C(t)| \to 0$ as $|\boldsymbol{x}(t) - \boldsymbol{x}^C(t)| \to 0$, where $\|(\cdot)\|$ denotes the matrix norm of $(\cdot)$. Thus the performance index is arbitrarily close to the infimum, *i.e.*, $\Delta V \to 0$ for sufficiently large n and t.

References

[1] D. W. Dunham, Contingency plans for the isee-3 libration-point mission, in: AIAA/AAS Astrodynamics Specialist Conference, AIAA Paper 79-129, AIAA/AAS, 1979.

[2] D. W. Dunham, S. J. Jen, C. E. Roberts, A. W. Seacord, P. J. Sharer, D. C. Folta, D. P. Muhonen, Transfer trajectory design for the soho libration-point mission, in: 43rd Congress of the International Astronautical Federation Congress, Washington, Distinct of Columbia, Paper IAF 92-0066, 1992.

[3] G. Gómez, A. Jorba, J. Llibre, R. Martínez, J. Masdemont, C. Simó, Dynamics and Mission Design Near Libration Points, Vol. I-IV, World Scientific, Singapore, 2001.

[4] C. L. Bennett, M. Halpern, G. Hinshaw, N. Jarosik, M. Limon, J. Mather, S. S. Meyer, L. Page, D. N. Spergel, G. Tucker, et al., The microwave anisotropy probe (map) mission, Vol. 29, AAS Paper 88.05, American Astronomical Society, 1997, p. 1391.

[5] B. T. Barden, K. C. Howell, M. W. Lo, Application of dynamical systems theory to trajectory design for a libration point mission, Journal of the Astronautical Sciences 45 (2) (1997) 161–178.

[6] M. W. Lo, B. G. Williams, W. E. Bollman, D. Han, Y. Hahn, J. L. Bell, E. A. Hirst, R. A. Corwin, P. Hong, K. C. Howell, et al., Genesis mission design, Journal of the Astronautical Sciences 49 (1) (2001) 169–184.

[7] E. Belbruno, J. Miller, A ballistic lunar capture trajectory for the japanese spacecraft hiten, Jet Propulsion Laboratory, IOM 312 (1990) 90–4.

[8] K. Uesugi, H. Matsuo, J. Kawaguchi, T. Hayashi, Japanese first double lunar swingby mission 'hiten', Acta Astronautica 25 (7) (1991) 347–355.

[9] B. H. Foing, G. R. Racca, The ESA smart-1 mission to the moon with solar electric propulsion, Advances in Space Research 23 (11) (1999) 1865–1870.

[10] S. B. Broschart, M.-K. J. Chung, S. J. Hatch, J. H. Ma, T. H. Sweetser, S. S. Weinstein-Weiss, V. Angelopoulos, Preliminary trajectory design for the artemis lunar mission, Advances in the Astronautical Sciences 135 (2) (2009) 1329–1343.

[11] R. S. Smith, F. Y. Hadaegh, Control of deep-space formation-flying spacecraft; relative sensing and switched information, Journal of Guidance Control and Dynamics 28 (1) (2005) 106–114.

[12] M. Zhu, H. R. Karimi, H. Zhang, Q. Gao, Y. Wang, Active disturbance rejection station-keeping control of unstable orbits around collinear libration points, Mathematical Problems in Engineering 2014 (2014) 1–14.

[13] Y. Ulybyshev, Long-term station keeping of space station in lunar halo orbits, Journal of Guidance, Control, and Dynamics 38 (6) (2015) 1063–1070.

[14] M. Shirobokov, S. Trofimov, M. Ovchinnikov, Survey of station-keeping techniques for libration point orbits, Journal of Guidance, Control, and Dynamics 40 (2017) 1085–1105.

[15] D. W. Dunham, C. E. Roberts, Stationkeeping techniques for libration-point satellites, The Journal of the astronautical sciences 49 (1) (2001) 127–144.

[16] J. V. Breakwell, A. A. Kamel, M. J. Ratner, Station-keeping for a translunar communication station, Celestial Mechanics 10 (3) (1974) 357–373.

[17] C. Simó, G. Gómez, J. Llibre, R. Martinez, J. Rodriguez, On the optimal station keeping control of halo orbits, Acta Astronautica 15 (6-7) (1987) 391–397.

[18] K. C. Howell, H. J. Pernicka, Station-keeping method for libration point trajectories, Journal of Guidance, Control, and Dynamics 16 (1) (1993) 151–159.

[19] G. Gómez, A. Jorba, J. Llibre, R. Martínez, C. Simó, Dynamics and Mission Design Near Libration Points: Volume I: Fundamentals: The Case of Collinear Libration Points, Vol. 2, World Scientific, 2001.

[20] D. C. Folta, M. Woodard, T. Pavlak, A. Haapala, K. C. Howell, Earth-moon libration stationkeeping: Theory, modeling, and operations, Advances in the Astronautical Sciences 145 (2012) 489–507.

[21] D. C. Folta, T. A. Pavlak, A. F. Haapala, K. C. Howell, M. A. Woodard, Earth–moon libration point orbit stationkeeping: Theory, modeling, and operations, Acta Astronautica 94 (1) (2014) 421–433.

[22] D. J. Scheeres, F.-Y. Hsiao, N. X. Vinh, Stabilizing motion relative to an unstable orbit: Applications to spacecraft formation flight, Journal of Guidance, Control, and Dynamics 26 (1) (2003) 62–73.

[23] H. Peng, J. Zhao, Z. Wu, W. Zhong, Optimal periodic controller for formation flying on libration point orbits, Acta Astronautica 69 (7) (2011) 537–550.

[24] P. Gurfil, N. J. Kasdin, Dynamics and control of spacecraft formation flying in three-body trajectories, in: AIAA Guidance, Navigation, and Control Conference and Exhibit, Montreal, Canada, 2001.

[25] A. Saberi, P. Sannuti, A. Stoorvogel, Control of Linear Systems with Regulation and Input Constraints, Springer-Verlag, Berlin, 2000.

[26] M. Bando, A. Ichikawa, Formation flying along halo orbit of circular-restricted three-body problem, Journal of Guidance, Control, and Dynamics 38 (1) (2015) 123–129.

[27] Y. Akiyama, M. Bando, S. Hokamoto, Station-keeping and formation flying for periodic orbit around lagrangian points by fourier series, in: International Symposium on Space Flight Dynamics, German Space Operations Center and ESA's European Space Operations Centre Munich, Germany, 2015.

[28] A. Isidori, C. I. Byrnes, Output regulation of nonlinear systems, IEEE Transactions on Automatic Control 35 (2) (1990) 131–140.

[29] H. Suzuki, N. Sakamoto, S. Celikovskỳ, Analytical approximation method for the center manifold in the nonlinear output regulation problem, in: 47th IEEE Conference on Decision and Control, Institute of Electrical and Electronics Engineers, 2008, pp. 1163–1168.

[30] B. Wie, Space Vehicle Dynamics and Control, AIAA Education Series, Reston, VA, 1998.